Applied Physics Letters

Non-conventional bell-shaped diffuse scattering in low-energy electron diffraction from high-quality epitaxial 2D-materials

Cite as: Appl. Phys. Lett. **118**, 241902 (2021); https://doi.org/10.1063/5.0051220
Submitted: 23 March 2021 . Accepted: 31 May 2021 . Published Online: 16 June 2021

K. Omambac, M. Kriegel, C. Brand, et al.

Applied Physics Letters ARTICLE scitation.org/journal/apl

Non-conventional bell-shaped diffuse scattering in low-energy electron diffraction from high-quality epitaxial 2D-materials

Cite as: Appl. Phys. Lett. **118**, 241902 (2021); doi: 10.1063/5.0051220
Submitted: 23 March 2021 · Accepted: 31 May 2021 ·
Published Online: 16 June 2021

K. Omambac,[1] M. Kriegel,[1] C. Brand,[1] B. Finke,[1] L. Kremeyer,[1] H. Hattab,[1] D. Janoschka,[1] P. Dreher,[1] F.-J. Meyer zu Heringdorf,[1,2] D. Momeni Pakdehi,[3] K. Pierz,[3] H. W. Schumacher,[3] M. Petrović,[4] A. van Houselt,[5] B. Poelsema,[5] M. C. Tringides,[6,7] and M. Horn-von Hoegen[1,2,a)]

AFFILIATIONS

[1]Faculty of Physics, University of Duisburg-Essen, Lotharstrasse. 1, 47057 Duisburg, Germany
[2]Center for Nanointegration Duisburg-Essen (CENIDE), University of Duisburg-Essen, Carl-Benz-Str. 199, 47057 Duisburg, Germany
[3]Physikalisch-Technische Bundesanstalt, Bundesallee 100, 38116 Braunschweig, Germany
[4]Center of Excellence for Advanced Materials and Sensing Devices, Institute of Physics, Bijenička cesta 46, HR-10000 Zagreb, Croatia
[5]Physics of Interfaces and Nanomaterials, MESA+ Research Institute, University of Twente, Drienerlolaan 5, 7522 NB Enschede, The Netherlands
[6]Ames Laboratory—U.S. Department of Energy, Ames, Iowa 50011, USA
[7]Department of Physics and Astronomy, Iowa State University, Ames, Iowa 50011, USA

[a)]**Author to whom correspondence should be addressed:** michael.horn-von-hoegen@uni-due.de

ABSTRACT

A broad, bell-shaped intensity component is observed in low-energy electron diffraction from high-quality epitaxial 2D-systems. Three 2D-systems, graphene on Ir(111), graphene on SiC(0001), and hexagonal boron nitride on Ir(111), have been prepared *in situ* under ultra-high vacuum conditions. In all three systems—independent of substrate material—similar strong diffuse intensity is observed, exhibiting a width as large as 50% of the Brillouin zone and an integrated intensity more than 10 times the intensity of the Bragg spots. The presented experimental results provide evidence for a common origin of such diffuse diffraction intensity in different atomically thin 2D-materials.

A new and surprising finding for the well investigated 2D-material system graphene on SiC(0001) recently attracted attention: the observation of a pronounced, very broad and bell-shaped component (BSC) in low-energy electron diffraction (LEED).[1] In general, diffuse intensity in diffraction is attributed to disorder or defects.[2–5] In this case, however, the BSC has been attributed to the scattering of the low-energy electrons by the spatially extremely confined electrons within the 2D-layer.[1] The BSC exhibits a full width at half maximum (FWHM) of ∼50% of the surface Brillouin zone (i.e., 100%SBZ $\triangleq 4\pi/\sqrt{3}a_0$ corresponds to the distance between integer order spots for a hexagonal surface unit cell with lattice parameter a_0) and is, thus, covering significant portions of the LEED pattern. This strong diffuse background does not originate from disorder or defects as the BSC has been observed even for the highest quality graphene films with micrometer-sized single crystalline grains.[6]

In this Letter, we report on the observation of a strong BSC in spot profile analysis (SPA)-LEED for three different high-quality 2D-material/substrate systems, namely, graphene on Ir(111), graphene on SiC(0001), and hexagonal boron nitride (hBN) on Ir(111). Although these material combinations include graphene on a metal, on a wide-bandgap semiconductor, and a bi-elemental 2D-material on a metal, we observe for all three systems a strong BSC with similar very large FWHM and large integrated intensity, i.e., the diffracted electrons 2D-integrated over the area of the spot in the 2-dimensional reciprocal space. This finding from such widely different systems supports a common origin for the BSC and proves that it is a unique property of uniform 2D-materials.

The experiments have been performed under ultra-high vacuum conditions at a base pressure of 2×10^{-10} mbar using high-resolution SPA-LEED for investigation of the BSC. SPA-LEED provides superior

signal-to-noise ratio of peak intensity in Bragg spots compared to typical diffuse background intensity and is, therefore, ideally suited for quantitative analysis of the BSC.[7–9] All LEED patterns were taken at room temperature. We have chosen an electron energy of $E = 69$ eV where intense spots and low background intensity of the initial non-graphitized substrates are observed. The background was further reduced by using the retarding field analyzer of the SPA-LEED with an energy resolution of $\Delta E = 0.5$ eV at $E = 69$ eV. All patterns are represented using a logarithmic intensity scale. All samples were prepared *in situ*.

Ir(111) substrates were cleaned by sputter annealing followed by a final annealing stepup to 1250 °C for 20 min. Sharp LEED spots and very low background intensity [see Fig. 1(a)] are indicative of a flat surface with low step density. Graphene was grown on Ir(111) by catalytic decomposition of ethylene at 1250 °C at a partial pressure of 5×10^{-6} mbar for an exposure time of 90 s. The growth is self-limiting to single layer graphene.[10] After exposure, the entire surface was covered with graphene exhibiting large domains as proven by low-energy electron microscopy (LEEM).[11,12] The LEED pattern shown in Fig. 1(b) demonstrates the growth of the oriented R0 phase with very little azimuthal disorder. We use "R0" to denote graphene with a unit cell oriented along the Ir(111) unit cell, i.e., alignment of Ir dense-packed rows with the zigzag direction of graphene.[13,14] The intense moiré pattern indicates the formation of monolayer graphene.[15]

Graphene on SiC(0001) was grown through *in situ* annealing of 4H-SiC(0001).[16,17] Degassing of the samples at 600 °C for 1 h resulted in clear (1×1) spots from the SiC(0001) substrate. After annealing at ∼950 °C for 1 min, the surface was transformed to a carbon rich $(\sqrt{3} \times \sqrt{3})$R30 reconstruction. Further annealing at ∼1100 °C for 30 s resulted in a $(6\sqrt{3} \times 6\sqrt{3})$R30 LEED pattern, indicating the formation of the carbon buffer layer.[18,19] Upon a final annealing step at 1200–1300 °C, a mixture of buffer layer and single layer graphene formed.[18] This situation is shown in the LEED pattern in Fig. 1(c). In addition, we also used 6H-SiC(0001) samples that were prepared *ex situ* in a furnace and that exclusively exhibited single layer graphene.[20,21] These samples were clamped on a Si wafer for transfer and degassing in ultra-high vacuum. Annealing at 650 °C for 10 min at a pressure below 1×10^{-9} mbar again resulted in sharp diffractions spots on a prominent BSC.

Epitaxial hBN films were grown by self-limiting catalytic decomposition of borazine ($B_3H_6N_3$) on Ir(111) at 850 °C for 90 s at a partial pressure of 5×10^{-8} mbar.[22,23] The sharp spots in the LEED pattern shown in Fig. 1(d) reflect the growth of the oriented R0 phase without azimuthal disorder. Large domains of micrometer size covering more than 90% of the surface were verified by *ex-situ* AFM and *in situ* LEEM.

For further characterization of the BSC, we recorded spot profiles that are plotted in a logarithmic intensity scale as gray data points in the left panels of Fig. 1. The profiles were recorded through the (00)-spot along the direction toward the next integer order spots of the surface Brillouin zone of the substrate, i.e., along the $[11\bar{2}]$ direction for Ir(111) and $[2\bar{1}\bar{1}0]$ direction for SiC(0001), respectively. Fitting the data (red curves) allows deconstructing the intensity profiles into their individual contributions (black curves) and provides a quantitative measure of the contribution of the BSC to the LEED pattern. The Bragg peaks for the 2D-materials were all fitted by Voigt functions to account for the instrumental resolution and finite size effects arising from step size distributions of the substrate into account.[8,9] The BSC is well described by a Gaussian profile for all of the 2D-materials investigated. We note that a fit with a Lorentzian profile or Moffat distribution yields systematic deviations on the flanks of the BSC.

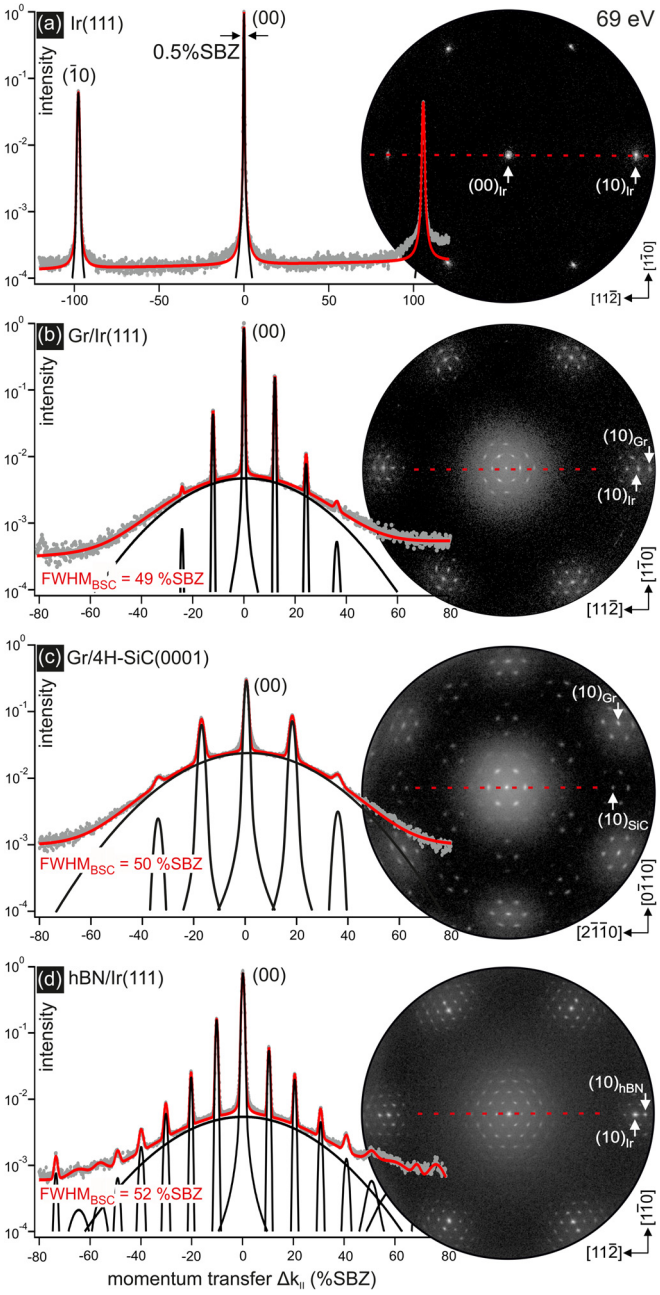

FIG. 1. LEED patterns and intensity line profiles across the first BZ and through the (00) spot at $E = 69$ eV. (a) The bare Ir(111) surface, (b) graphene on Ir(111), (c) graphene on 4H-SiC(0001), and (d) hBN on Ir(111). Spot profiles on the Ir substrate are taken along the $[11\bar{2}]$ direction and on SiC(0001) along the $[2\bar{1}\bar{1}0]$ direction. Gray dots indicate data points, and the red lines are fits to the data, which are composed of individual components shown as black lines. The LEED patterns are shown using a logarithmic intensity scale with arbitrary units.

The spot profile of the bare Ir(111) surface in Fig. 1(a) shows the (00)-spot and the first integer order spots. From the narrow FWHM of these spots of 0.5%SBZ, we conclude that this is only due to instrumental broadening and a coherence length at the surface of 60 nm. The ratio of the intensities of the (00)-spot and the diffuse thermal background is 5×10^3:1. This rather large value is indicative for the high quality of the Ir(111) substrate with a low step density and without small-angle mosaic spread.[8,9]

The spot profiles of the three investigated 2D-systems are shown in the left panels of Figs. 1(b)–1(d). They are all composed of a (00)-spot, moiré or superlattice spots, the BSC, and a low constant background intensity.

The LEED pattern of Gr/Ir(111) in Fig. 1(b) is characterized by moiré spots up to third order surrounding all integer order spots. The moiré spots arise from the approximate 10 to 9 ratio of the graphene to Ir lattice constant.[10,24] The large number of clearly visible moiré spots and the single azimuthal orientation R0 are all indicators of the high quality of the grown graphene. The weak azimuthal wings of the moiré spots indicate slight azimuthal disorder, which is enlarged by one order of magnitude by the moiré magnifying effect. Such disorder has been observed for sufficiently large single crystalline graphene domains in LEEM[35] and may be inevitable due to wrinkle formation upon cooling.[15,24]

The prominent broad and isotropic diffuse intensity of the BSC surrounds the (00)-spot and all integer order spots of graphene. The BSC at the first order spots is not centered at the Ir spots but on the graphene spots,[24] which confirms that the BSC is related to the graphene layer rather than being a substrate effect.[1]

The BSC of the (00)-spot is well described by a Gaussian profile with a FWHM of 49 %SBZ of the Ir(111) substrate, i.e., 1.31 $Å^{-1}$. Comparing the total 2D-integrated intensity of the BSC to the total integrated intensity of the sum of the (00)-spot and all of its moiré spots, we obtain a ratio ($\int I_{00} + \Sigma \int I_{\text{moiré}}$): $\int I_{\text{BSC}} = 1{:}20$, i.e., the BSC exhibits one order of magnitude more scattered electrons than the Bragg spots. All the moiré spots surrounding the (00)-spots are included in finding the ratio of BSC to Bragg spot integrated intensities. In any case, the analysis shows that the sum over all moiré spots exhibits a total 2D-integrated intensity comparable to the 2D-integrated intensity of the (00)-spot, which does not affect the primary conclusion that the BSC intensity is at least one order of magnitude larger than the one from the Bragg spots.

The results for Gr/SiC(0001) are shown in Fig. 1(c). The LEED pattern is dominated by the dense array of $(6\sqrt{3} \times 6\sqrt{3})$ superstructure spots arising from the graphene-covered buffer layer.[18,19] The integer order spots of the graphene layer are rotated by 30° with respect to the SiC(0001) substrate.[16] These spots clearly show a significant BSC. The integer order spots from the SiC(0001) substrate do not exhibit any BSC. Like in the graphene/Ir(111) case outlined above, this result unambiguously shows that the origin of the BSC can only be found in the 2D-layer.

Again, the fit to the BSC of the (00)-spot yields a Gaussian profile with a FWHM of 53 %SBZ of the substrates surface Brillouin zone (here referenced to the 4H-SiC(0001) substrate), i.e., 1.25 $Å^{-1}$. We yield a ratio of the integrated intensities of the Bragg peaks to the BSC component ($\int I_{00} + \Sigma \int I_{6\sqrt{3}}$): $\int I_{\text{BSC}} = 1{:}14$.

The results for hBN/Ir(111) are shown in Fig. 1(d). The LEED pattern is again dominated by intense and narrow moiré spots up to fifth order that surround all integer order spots. The intense moiré spots also indicate the high quality and large lateral extent of the grown hBN domains.[36] The moiré spots arise from the approximate 11 to 10 ratio of the hBN to Ir(111) lattice parameter.[23] The broad and isotropic diffuse intensity of the BSC is clearly visible, surrounding the (00)-spot and all integer order spots of the 2D-layer. Again, the BSC of the first integer order spots is centered at the hBN spots and not at the Ir spots. The BSC of the (00)-spot has been fitted by a Gaussian profile with a FWHM of 52 %SBZ [referenced to the Ir(111) substrate], i.e., 1.39 $Å^{-1}$. Again, the ratio of Bragg and BSC integrated intensities is very low (1:12). The results are summarized in Table I.

Our results show that BSC is a very prominent feature in electron diffraction of different 2D-material systems and that their presence is not only limited to graphene on SiC(0001).[1,6] Surprisingly, our quantitative analysis reveals that the extracted parameters (integrated intensity and FWHM) are very similar across different 2D-material systems, as summarized in Table I. This implies that the mechanism causing the BSC must be very general and of fundamental nature. The origin of the BSC should be independent of the chemical composition and the underlying substrate, but at the same time, it should also be present in 2D-systems of high uniformity and superior quality.

Not many mechanisms can be relevant under such widely diverse material properties. However, it is worth examining whether plasmons excited in the 2D-material by the incident electron beam might be relevant to the origin of the BSC. Plasmons are longitudinal electron-density waves formed parallel to the surface by the conduction electrons and exhibit well-defined dispersion relations.

Both, graphene on SiC(0001) and Ir(111), possess conduction electrons because substrate mediated doping shifts the Fermi level away from the Dirac point. Such plasmonic excitations in graphene/Ir(111) were, for instance, studied in Refs. 25 and 26. The plasmon energy increases monotonically with its momentum. As evident from the dispersion relation in Fig. 5 of Ref. 25, even for plasmon wavevectors of only 10%SBZ the plasmon energy is already 1.0 eV, i.e., large enough to be filtered by the SPA-LEED retarding field analyzer with 0.5 eV resolution. Such energy filtering is also effective for higher-energy plasmons with wavevectors comparable to the large k-space extension of the BSC.

Regarding hBN, photoluminescence measurements show that pristine hBN is an insulator with a bandgap of ∼6 eV[27] and, thus, delocalized charge carriers do not exist. For 2D-hBN on a metal

TABLE I. Parameters of the bell-shaped component (BSC) for three different material systems. FWHM of the Gaussian profile of the BSC is given in both % of surface Brillouin zone of the respective substrate and in inverse angstrom. The ratio of integrated intensities of the (00) spot to the BSC and all Bragg spots to the BSC are given for the first SBZ.

	Graphene/ Ir(111)	Graphene/ SiC(0001)	hBN/Ir(111)
FWHM of BSC	49 $\%SBZ_{Ir(111)}$ 1.31 $Å^{-1}$	53 $\%SBZ_{SiC(0001)}$ 1.25 $Å^{-1}$	52 $\%SBZ_{Ir(111)}$ 1.39 $Å^{-1}$
$\int I_{00} : \int I_{\text{BSC}}$	1:40	1:52	1:21
$(\int I_{00} + \Sigma \int I_{\text{moiré}}) : \int I_{\text{BSC}}$	1:20	1:14	1:12

substrate, however, the interaction with the substrate reduces the bandgap.[28] A finite but small carrier density is, thus, most likely present. Even with the presence of delocalized carriers in doped samples, similar conclusions should hold as for plasmons in graphene. Thus, plasmons cannot contribute to the BSC in all three discussed 2D-materials.

Our quantitative diffraction study reveals that in addition to graphene on different substrates, hBN also exhibits a strong bell-shaped component in low-energy electron diffraction. The quantitative analysis shows that the extracted intensity ratios and FWHMs are very similar for all substrates and 2D-materials used. In all discussed cases, the BSC spans across half of the surface Brillouin zone, and its integrated intensity is at least one order of magnitude larger than the integrated intensity of the Bragg component. The BSC must originate exclusively from the 2D-material as it is replicated and centered at all integer order spots of the 2D-layer—also in the case of the 30° rotated graphene on SiC(0001).

Numerous studies of other groups have revealed the presence of a BSC in diffraction patterns from 2D-materials, although this strong effect was never mentioned.[1] A quantification of its properties or discussion of its potential origin was lacking. Through our comprehensive study of three different 2D-material systems, we are able to exclude plasmons as origin for the BSC; thus, an alternative explanation for the BSC is needed. Chen *et al.* suggested the confinement of the electrons in the π-bonds of the 2D-layer within the interlayer spacing of $d \sim 3.3$ Å as a plausible but preliminary explanation of the BSC. The confinement generates a spread in the normal component of the wavevector of the confined carriers $\Delta\kappa_z \sim 1/d$ as measured by angle resolved photo-emission.[29] This momentum spread is transferred to the incoming low-energy electrons and, after diffraction, generates the BSC.[1] In line with this, graphite that has macroscopic thickness and an "infinite" number of graphene layers, does not show the BSC.[30]

Independent of the origin of the BSC, we note that in the three systems investigated here, the diffraction patterns exhibit very narrow fundamental substrate spots, a large number of sharp moiré spots, and in Fig. 1(a) only slight azimuthal disorder. In other Gr/Ir(111) studies—when further annealing eliminates azimuthal disorder and only the R0 graphene orientation remains—the BSC is also maximal.[13] This evidences high crystallinity, single orientation, and low defect density in the examined 2D-materials when growth conditions are optimized. In the systems under investigation, the BSC has been proven to be isotropic without any azimuthal variation of shape or width.

The presence of very broad diffuse LEED intensity has been studied before. It was discussed in terms of point defects and it was analyzed to extract the type and extent of disorder present on the surface.[31–33] However, 2D-integrated intensity as strong as in our data has never been observed before and would require more than half of the atomic sites to be occupied by defects, which contradicts the findings from numerous STM studies on these systems.

The presence of a strong BSC is, thus, not related to defects within the 2D-materials but is an inherent feature of these atomically thin systems.[34] As such, observing a pronounced BSC may be simply evidence for a high-quality uniform and homogeneous film. Hopefully, our surprising findings will motivate more BSC studies in other 2D-materials and more theoretical work to provide a comprehensive understanding of the mechanism behind such paradoxical results.

AUTHORS' CONTRIBUTIONS

All authors contributed equally to the work and manuscript.

Funding by the Deutsche Forschungsgemeinschaft (DFG, German Research Foundation) through projects B04 and B06 of Collaborative Research Center SFB1242 "Non-equilibrium dynamics of condensed matter in the time domain" (Project No. 278162697) is appreciated. Support by the Interdisciplinary Center for Analytics on the Nanoscale (ICAN) of the University of Duisburg-Essen, a DFG funded core facility (DFG Resources reference: RI_00313, Grant No. HA 2769/7–1), is gratefully acknowledged. M.P. acknowledges financial support from the Alexander von Humboldt Foundation and from the Center of Excellence for Advanced Materials and Sensing Devices (ERDF Grant No. K.01.1.1.01.0001). H.H. acknowledges financial support from the Deutsche Akademie der Naturforscher Leopoldina through a Leopoldina Postdoc Scholarship. This work was partially supported by the U.S. Department of Energy (DOE), Office of Science, Basic Energy Sciences, Materials Sciences and Engineering Division. Part of the Research was performed at the Ames Laboratory, which is operated by Iowa State University under Contract No. DE-AC02–07CH11358.

DATA AVAILABILITY

The data that support the findings of this study are available from the corresponding author upon reasonable request.

REFERENCES

[1]S. Chen, M. Horn von Hoegen, P. A. Thiel, and M. Tringides, "A diffraction paradox: An unusually broad diffraction background marks high quality graphene," Phys. Rev. B **100**, 155307 (2019).
[2]M. Henzler, "LEED-investigation of step arrays on cleaved germanium (111) surfaces," Surf. Sci. **19**, 159 (1970).
[3]M. Henzler, "Quantitative evaluation of random distributed steps at interfaces and surfaces," Surf. Sci. **73**, 240 (1978).
[4]M. Henzler, "LEED studies of surface imperfections," Appl. Surf. Sci. **11–12**, 450 (1982).
[5]M. Henzler, "Measurement of surface defects by low-energy electron diffraction," Appl. Phys. A **34**, 205 (1984).
[6]S. Chen, M. Horn von Hoegen, P. A. Thiel, A. Kaminski, B. Schrunk, T. Speliotis, E. H. Conrad, and M. C. Tringides, "High layer uniformity of two-dimensional materials demonstrated surprisingly from broad features in surface electron diffraction," J. Phys. Chem. Lett **11**, 8937 (2020).
[7]U. Scheithauer, G. Meyer, and M. Henzler, "A new LEED instrument for quantitative spot profile analysis," Surf. Sci. **178**, 441 (1986).
[8]M. Horn-von Hoegen, "Growth of semiconductor layers studied by spot profile analysing low energy electron diffraction—Part I," Z. Kristallogr. **214**, 591 (1999).
[9]M. Horn-von Hoegen, "Growth of semiconductor layers studied by spot profile analysing low energy electron diffraction—Part II," Z. Kristallogr. **214**, 684 (1999).
[10]J. Coraux, A. T N'Diaye, M. Engler, C. Busse, D. Wall, N. Buckanie, F.-J. Meyer zu Heringdorf, R. van Gastel, B. Poelsema, and T. Michely, "Growth of graphene on Ir(111)," New J. Phys. **11**, 039801 (2009).
[11]R. van Gastel, A. T. N'Diaye, D. Wall, J. Coraux, C. Busse, N. M. Buckanie, F.-J. Meyer zu Heringdorf, M. Horn-von Hoegen, T. Michely, and B. Poelsema, "Selecting a single orientation for millimeter sized graphene sheets," Appl. Phys. Lett. **95**, 121901 (2009).
[12]R. Besson, M. Rocha Vargas, and L. Favergeon, "CO_2 adsorption on calcium oxide: An atomic-scale simulation study," Surf. Sci. **606**, 490 (2012).
[13]H. Hattab, A. T. N'Diaye, D. Wall, G. Jnawali, J. Coraux, C. Busse, R. van Gastel, B. Poelsema, T. Michely, F.-J. Meyer zu Heringdorf, and M. Horn-von

Hoegen, "Growth temperature dependent graphene alignment on Ir(111)," Appl. Phys. Lett. **98**, 141903 (2011).
[14]K. M. Omambac, H. Hattab, C. Brand, G. Jnawali, A. T. N'Diaye, J. Coraux, R. von Gastel, B. Poelsema, T. Michely, F.-J. Meyer zu Heringdorf, and M. Horn-von Hoegen, "Temperature-controlled rotational epitaxy of graphene," Nano Lett. **19**, 4594 (2019).
[15]A. T. N'Diaye, R. van Gastel, G. Martinez, J. Coraux, H. Hattab, F.-J. Meyer zu Heringdorf, D. Wall, M. Horn-von Hoegen, J.-M. Gomez-Rodriguez, B. Poelsema, C. Busse, and T. Michely, "In situ observation of stress relaxation in epitaxial graphene," New J. Phys. **11**, 113056 (2009).
[16]C. Berger, Z. Song, T. Li, X. Li, A. Y. Ogbazghi, R. Feng, Z. Dai, A. N. Marchenkov, E. H. Conrad, P. N. First, and W. A. de Heer, "Ultrathin epitaxial graphite: 2D electron gas properties and a route toward graphene-based nanoelectronics," J. Phys. Chem. B **108**, 19912 (2004).
[17]K. V. Emtsev, A. Bostwick, K. Horn, J. Jobst, G. L. Kellogg, L. Ley, J. L. McChesney, T. Ohta, S. A. Reshanov, J. Röhrl, E. Rotenberg, A. K. Schmid, D. Waldmann, H. B. Weber, and T. Seyller, "Towards wafer-size graphene layers by atmospheric pressure graphitization of silicon carbide," Nat. Mater. **8**, 203 (2009).
[18]C. Riedl, U. Starke, J. Bernhardt, M. Franke, and K. Heinz, "Structural properties of the graphene-SiC(0001) interface as a key for the preparation of homogeneous large-terrace graphene surfaces," Phys. Rev. B **76**, 245406 (2007).
[19]T. Langer, H. Pfnür, H. W. Schumacher, and C. Tegenkamp, "Graphitization process of SiC(0001) studied by electron energy loss spectroscopy," Appl. Phys. Lett. **94**, 112106 (2009).
[20]M. Kruskopf, D. Momeni Pakdehi, K. Pierz, S. Wundrack, R. Stosch, T. Dziomba, M. Götz, J. Baringhaus, J. Aprojanz, C. Tegenkamp, J. Lidzba, T. Seyller, F. Hohls, F. J. Ahlers, and H. W. Schumacher, "Comeback of epitaxial graphene for electronics: Large-area growth of bilayer-free graphene on SiC," 2D Mater. **3**, 041002 (2016).
[21]D. Momeni Pakdehi, K. Pierz, S. Wundrack, J. Aprojanz, T. T. N. Nguyen, T. Dziomba, F. Hohls, A. Bakin, R. Stosch, C. Tegenkamp, F. J. Ahlers, and H. W. Schumacher, "Homogeneous large-area quasi-free-standing monolayer and bilayer graphene on SiC," ACS Appl. Nano Mater. **2**, 844 (2019).
[22]F. H. Farwick zum Hagen, D. M. Zimmermann, C. C. Silva, C. Schlueter, N. Atodiresei, W. Jolie, A. J. Martínez-Galera, D. Dombrowski, U. A. Schröder, M. Will, P. Lazić, V. Caciuc, S. Blügel, T.-L. Lee, T. Michely, and C. Busse, "Structure and growth of hexagonal boron nitride on Ir(111)," ACS Nano **10**, 11012 (2016).
[23]D. Usachov, A. Fedorov, O. Vilkov, V. K. Adamchuk, L. V. Yashina, L. Bondarenko, A. A. Saranin, A. Grüneis, and D. V. Vyalikh, "Experimental and computational insight into the properties of the lattice-mismatched structures: Monolayers of h-BN and graphene on Ir(111)," Phys. Rev. B **86**, 155151 (2012).
[24]H. Hattab, A. T. N'Diaye, D. Wall, C. Klein, G. Jnawali, J. Coraux, C. Busse, R. van Gastel, B. Poelsema, T. Michely, F.-J. Meyer zu Heringdorf, and M. Horn-von Hoegen, "Interplay of wrinkles, strain, and lattice parameter in graphene layers on iridium," Nano Lett. **12**, 678 (2012).
[25]T. Langer, J. Baringhaus, H. Pfnür, H. W. Schumacher, and C. Tegenkamp, "Plasmon damping below the Landau regime: The role of defects in epitaxial graphene," New J. Phys. **12**, 033017 (2010).
[26]T. Langer, D. F. Förster, C. Busse, T. Michely, H. Pfnür, and C. Tegenkamp, "Sheet plasmons in modulated graphene on Ir(111)," New J. Phys. **13**, 053006 (2011).
[27]G. Cassabois, P. Valvin, and B. Gil, "Hexagonal boron nitride is an indirect bandgap semiconductor," Nat. Photonics **10**, 262 (2016).
[28]M. Liu, Y. Li, P. Chen, J. Sun, D. Ma, Q. Li, T. Gao, Y. Gao, Z. Cheng, X. Qiu, Y. Fang, Y. Zhang, and Z. Liu, "Quasi-freestanding monolayer heterostructure of graphene and hexagonal boron nitride on Ir(111) with a zigzag boundary," Nano Lett. **14**, 6342 (2014).
[29]T. Ohta, A. Bostwick, J. L. McChesney, T. Seyller, K. Horn, and E. Rotenberg, "Interlayer interaction and electronic screening in multilayer graphene investigated with angle-resolved photoemission spectroscopy," Phys. Rev. Lett. **98**, 206802 (2007).
[30]N. Ferralis, K. Pussi, S. E. Finberg, J. Smerdon, M. Lindroos, R. McGrath, and R. D. Diehl, "Low-energy electron diffraction study of potassium adsorbed on single-crystal graphite and highly oriented pyrolytic graphite," Phys. Rev. B **70**, 245407 (2004).
[31]W. Moritz, *Determination of Surface Structure by LEED*, edited by P. M. Marcus and F. Jona (Plenum Press, New York, 1984), p. 505.
[32]K. Heinz, D. K. Saldin, and J. B. Pendry, "Diffuse LEED and surface crystallography," Phys. Rev. Lett. **55**, 2312 (1985).
[33]P. J. Rous and J. B. Pendry, "Multiple scattering theory of diffuse LEED from vacancies," Surf. Sci. **155**, 241 (1985).
[34]C. Struzzi, N. I. Verbitskiy, A. V. Fedorov, A. Nefedov, O. Frank, M. Kalbac, G. D. Santo, M. Panighel, A. Goldoni, J. Gärtner, W. Weber, M. Weinl, M. Schreck, C. Wöll, H. Sachdev, A. Grüneis, and L. Petaccia, "High-quality graphene on single crystal Ir(111) films on Si(111) wafers: Synthesis and multispectroscopic characterization," Carbon **81**, 167 (2015).
[35]K. L. Man and M. S. Altman, "Small-angle lattice rotations in graphene on Ru(0001)," Phys. Rev. B **84**, 235415 (2011).
[36]M. Petrović, U. Hagemann, M. Horn-von Hoegen, and F.-J. Meyer zu Heringdorf, "Microanalysis of single-layer hexagonal boron nitride islands on Ir(111)," Appl. Surf. Sci. **420**, 504 (2017).